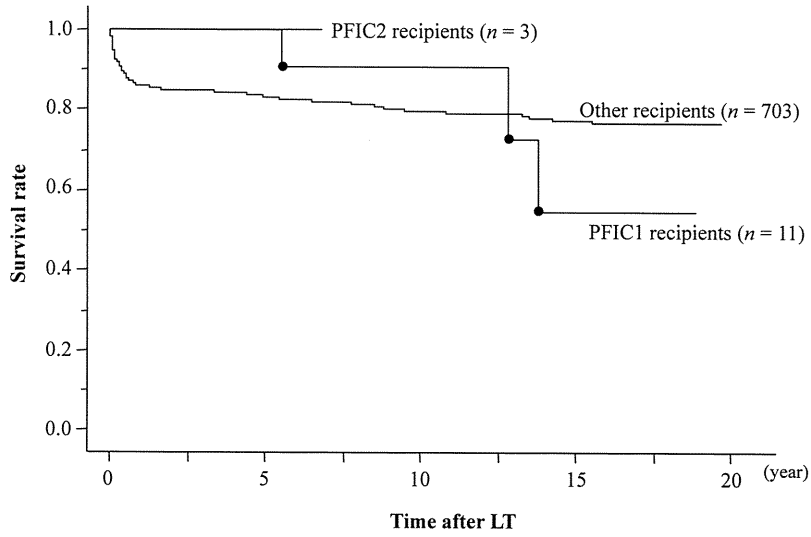

Fig. 1. Survival curves for PFIC1, PFIC2, and other recipients after living-donor liver transplantation (LDLT). The survival curves after LDLT in each of the 11 PFIC1 recipients, three PFIC2 recipients, and 703 other recipients were calculated by the Kaplan–Meier method. PFIC, progressive familial intrahepatic cholestasis.

Table 2. Histopathological findings after LDLT

Case number	PFIC	LNBs after LDLT (times)	Steatosis		Steatohepatitis	Fibrosis		Other histopathological findings after LDLT	Outcome (POD)
			LNB[a] (POD)	Percentage		LNB[a] (POD)	Score[b] (F)		
1	Type 1	10	378	90	+	2303	3	–	Alive (6884)
2	Type 1	6	–	0	–	4171	4	*De novo* AIH	Alive (6604)
3	Type 1	9	46	90	+	480	4	–	Dead (5032)
4	Type 1	4	–	0	–	–	0	–	Alive (5605)
5	Type 1	13	1305	80	+	1869	3	–	Dead (4671)
6	Type 1	8	138	80	+	468	3	–	Alive (4295)
7	Type 1	7	736	30	+	3254	4	–	Alive (4065)
8	Type 1	3	87	80	–	–	0	–	Alive (3384)
9	Type 1	11	397	90	+	991	3	–	Alive (3265)
10	Type 1	23	–	0	–	1125	4	Chronic rejection	Dead (2005)
11	Type 1	5	34	80	+	34	1	–	Alive (2028)
12	Type 2	4	–	0	–	–	0	–	Alive (2453)
13	Type 2	6	–	0	–	–	0	–	Alive (1601)
14	Type 2	7	–	0	–	–	0	Refractory ACR	Alive (500)

ACR, acute cellular rejection; AIH, autoimmune hepatitis; LDLT, living-donor liver transplantation; LNB, liver needle biopsy; NASH, nonalcoholic steatohepatitis; PFIC, progressive familial intrahepatic cholestasis; POD, postoperative day.
[a]The PODs of the peak findings are shown if the histopathological findings were positive. The earliest PODs are shown if the histopathological findings were equal.
[b]Fibrosis score: the NASH score was used for steatosis-positive recipients, while the METAVIR score was used for steatosis-negative recipients.

no fibrosis was confirmed in the PFIC2 recipients. Moreover, the steatosis and steatohepatitis that subsequently caused fibrosis were surprisingly confirmed even during the early post-operative period in these PFIC1 recipients.

Nine of 11 PFIC1 recipients showed fibrosis after LDLT (Cases 1–3, 5–7 and 9–11), whereas no fibrosis was confirmed in the remaining two PFIC1 recipients. Eight of the nine fibrosis-positive PFIC1 recipients showed F scores of ≥3 (Cases 1–3, 5–7, 9 and 10). The mean POD when the F score reached its peak was 1632.8 ± 1391.4 d (range, 34–4171 d). Among the nine F score-positive PFIC1 recipients, seven were complicated with steatosis (Cases 1, 3, 5–7, 9 and 11), and two had fibrosis without steatosis (F4) for another reason (*de novo* AIH and chronic rejection) (Cases 2 and 10). In contrast to the PFIC1 recipients, the PFIC2 recipients did not show any steatosis or fibrosis.

Total external biliary diversion (TEBD)

In one PFIC1 recipient (Case 10), TEBD was performed at retransplantation, although we had no experience of TEBD at initial LDLTs. However, we cannot confirm the effects of LDLT

accompanied by TEBD, because this patient suffered graft loss owing to an arterioportal shunt after the retransplantation.

In our institution, TEBD is performed as a hepatico-jejuno-cutaneostomy. An isolated jejunal interposition of 15–20 cm in length is made with the proper mesentery at a point 20 cm distant from Treitz's ligament. Next, hepatico-jejunostomy was made. The jejunal interposition is placed between the hepatic hilum and the skin. An end-stoma is made in the right lower quadrant of the abdominal wall.

Discussion

The combined considerations of clinical, biochemical, radiological and histological approaches including liver immunostaining and biliary lipid analyses help diagnosis of PFIC candidates. Clinical manifestations of each type of PFIC documented in these studies are summarized in Table 3.

Phenotypic findings and extrahepatic features have been described in PFIC1 (4–10). The hepatic histopathology is characterized by canalicular cholestasis and the absence of true ductular proliferation with only periportal biliary metaplasia of hepatocytes. PFIC1 is caused by mutations in the ATP8B1 gene (designated FIC1) (7). Adenosine triphosphate (ATP) is elaborated from adenosine diphosphate and phosphoric acid via ATPase, and the FIC1 gene, which encodes a P-type ATPase, is located on human chromosome 18. Some investigators have described that impaired FIC1 function results in substantial downregulation of farnesoid X receptor (FXR), a nuclear receptor involved in the regulation of BA metabolism, with subsequent downregulation of BSEP in the liver and upregulation of BA synthesis and the apical sodium bile salt (BS) transporter in the intestine (21). The possible mechanisms of BA overload in hepatocytes are highlighted in Fig. 2A. The extrahepatic features such as diarrhea, liver steatosis, and short

Table 3. Characteristic manifestations of PFIC

	PFIC1 (FIC1 deficiency) (Byler's disease)	PFIC2 (BSEP deficiency) (Byler's syndrome)	PFIC3 (MDR3 deficiency)
Inheritance	18q21-22	Autosomal recessive	Autosomal recessive
Age of onset	Neonatal period	Neonatal period	1 month–20 yr
Cholestasis	Chronic	Chronic	Chronic
Ductular proliferation	Absent	Absent	Absent
Progression to cirrhosis	Yes	Yes	Yes
Cutaneous pruritus	Severe	Severe	Moderate
Serum γ-GT activity	Normal	Normal	High
Serum cholesterol level	Normal	Normal	Normal
Serum PBA concentration	Very high	Very high	High
Bile composition	Low PBA concentration	Very low PBA concentration	Low phospholipid concentration
Gene (encoding protein)	Autosomal recessive	ABCB11 (BSEP)	ABCB4 (MDR3)
Chromosomal locus	ATP8B1 (FIC1)	2q24	7q21
Function of hereditary defect	Aminophospholipid translocase	BA secretion	Phosphatidylcholine secretion
Hepatocyte location	Canalicular membrane	Canalicular membrane	Canalicular membrane
Other sites of mRNA expression	Cholangiocytes Intestine Pancreas	None	None
Resultant functional defect	ATP-dependent Aminophospholipid translocase	ATP-dependent BA transport in bile	ATP-dependent Phosphatidylcholine translocation in bile
Histopathological findings	Canalicular cholestasis Absence of true ductular proliferation Periportal biliary metaplasia of hepatocytes Pronounced portal/lobular fibrosis Pronounced portal/lobular inflammation Hepatocellular necrosis Giant cell transformation Perturbed liver architecture	Canalicular cholestasis Absence of true ductular proliferation Severe lobular injury More pronounced lobular/portal fibrosis More pronounced lobular/portal inflammation More obvious hepatocellular necrosis More obvious giant cell transformation More perturbed liver architecture	Rare cholestasis True ductular proliferation Normal interlobular bile ducts Rare extensive portal fibrosis Mixed inflammatory infiltrate Rare biliary cirrhosis Slight giant cell transformation No biliary epithelium injury

ATP, adenosine triphosphate; BA, bile acid; BSEP, bile salt export pump; FIC1, familial intrahepatic cholestasis 1; γ-GT, gamma-glutamyltransferase; MDR3, multidrug resistant 3; PBA, primary bile acid; PFIC, progressive familial intrahepatic cholestasis.

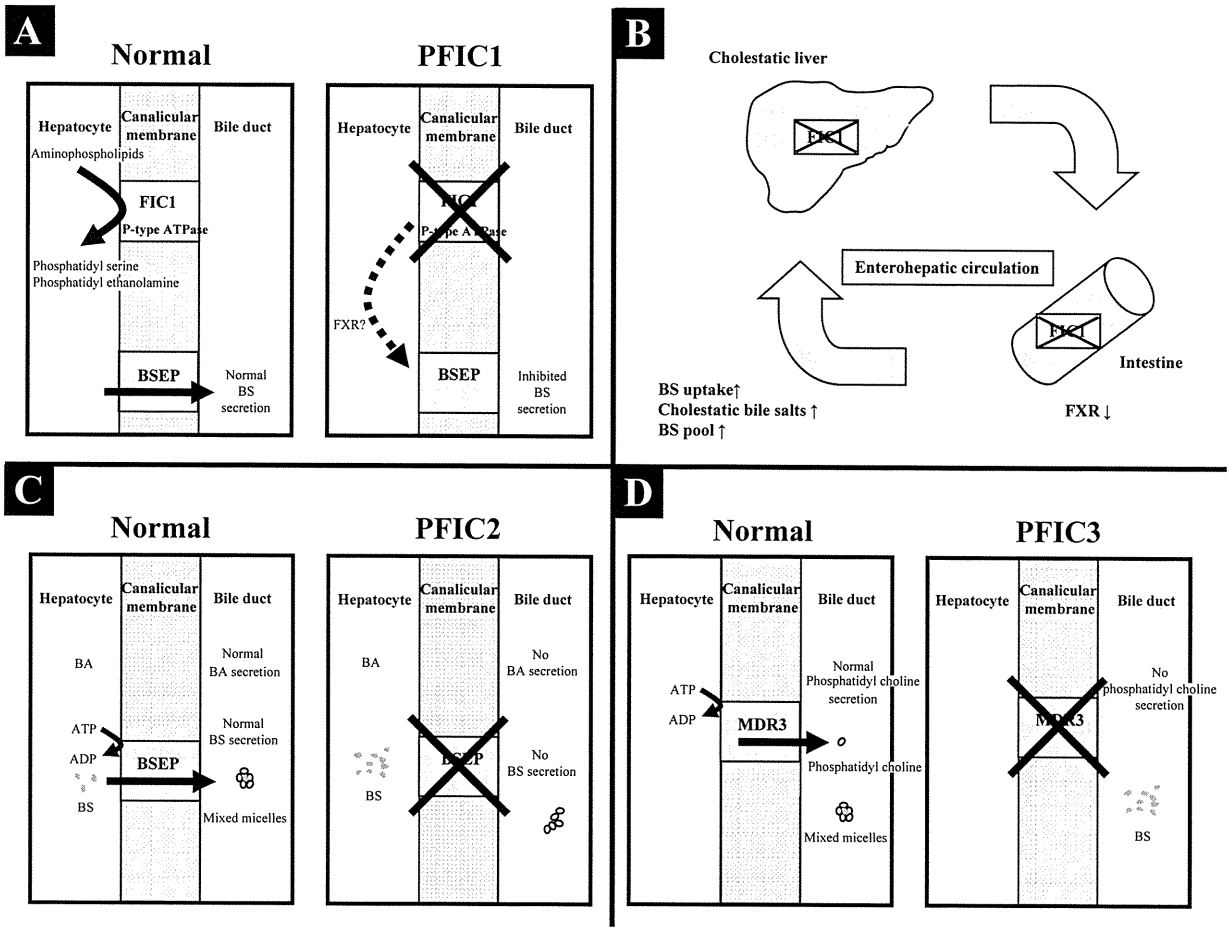

Fig. 2. Schemas of the mechanisms for the different types of progressive familial intrahepatic cholestasis (PFIC). (A) The possible mechanism of PFIC1. The FIC1 protein is located on the canalicular membrane of hepatocytes, but is mainly expressed in intrahepatic cholangiocytes. The function of the P-type ATPase is still unknown. However, it could be an aminophospholipid transporter responsible for maintaining the enrichment of phosphatidylserine and phosphatidylethanolamine on the inner leaflet of the plasma membrane. The asymmetric distribution of lipids in the membrane bilayer plays a protective role against high concentrations of bile salt (BS) in the canalicular lumen. The issue of how these mutations cause cholestasis remains unclear. It is postulated that abnormal protein function may indirectly disturb the biliary secretion of BA, thus explaining the low concentration of biliary BA. Impaired FIC1 function results in substantial downregulation of farnesoid X receptor (FXR), a nuclear receptor involved in the regulation of BA metabolism, with subsequent downregulation of bile salt export pump (BSEP) in the liver and upregulation of BA synthesis and the apical sodium BS transporter in the intestine. Eventually, these events lead to BA overload in hepatocytes. (B) Enterohepatic circulation in PFIC1. The downregulation of the cystic fibrosis transmembrane conductance regulator in cholangiocytes has been reported in PFIC1, and this downregulation could contribute to the impairment of bile secretion and explain some of the extrahepatic features. The FIC1 gene is expressed in various organs, including the liver, pancreas, small intestine and kidney, but is more highly expressed in the small intestine than in the liver. Therefore, enterohepatic cycling of BS should be considered in PFIC1. This may also explain the digestive symptoms including chronic diarrhea in PFIC1. Other extrahepatic features such as persistent short stature, deafness, and pancreatitis suggest a general cell biological function for FIC1. The downregulation of FXR in intestines is suggested in this pathway. (C) The mechanism of PFIC2. The BSEP protein, which is expressed on the hepatocyte canalicular membrane, is the major exporter of primary bile acid against extreme gradients of concentration. Mutations in this gene are responsible for decreased biliary BS secretion, which leads to decreased bile flow and accumulation of BS inside the hepatocytes, thereby resulting in severe hepatocellular damage. (D) The mechanism of PFIC3. The mechanism of the liver damage in PFIC3 is related to the absence of biliary phospholipids. The damage to the bile canaliculi and biliary epithelium probably results from continuous exposure to hydrophobic BSs, the detergent effects of which are no longer countered by phospholipids, thus leading to cholangitis. FIC1, familial intrahepatic cholestasis 1.

stature that are sometimes associated with PFIC1 do not improve or may be aggravated after successful biliary diversion or LT (1, 10). Chronic diarrhea may become intractable when biliary BS secretion is restored after LT (7, 10), while diarrhea may be favorably managed by bile adsorptive resin treatment (10). Similar to these previous reports, our data confirmed digestive symptoms after

LDLT in 10 of 11 PFIC1 recipients (91%), whereas the PFIC2 recipients showed no digestive symptoms. PFIC1 associated with severe liver steatosis and/or steatohepatitis may lead to cirrhosis over time, and to indications for retransplantation (1). However, liver steatosis and diarrhea may occur even after retransplantation (1). In LDLT, donor selection is very limited ethically, socially and medically. In Japan in particular, expansion of deceased-donor LT is not yet in sight, although the governmental legislation for organ transplantation was revised in 2009. There are no affirmations for repeated retransplantation that may collateralize the long-term outcomes of pediatric PFIC1 recipients. The outcomes of PFIC1 recipients after LDLT are still not sufficient, based on our data and a previous report (22). Our actual results for the early post-operative occurrences of steatosis and fibrosis oblige us to reconsider the timing of LDLT and to challenge some other therapies for PFIC1 patients. Previously, partial external biliary diversion (PEBD) has been documented as a surgical procedure for PFIC patients (23, 24). Some patients with PFIC1 or PFIC2 may also benefit from surgical biliary diversion (25–27). The criteria for identifying those PFIC1/2 patients who could benefit from UDCA or biliary diversion remain unclear (14). We clearly understand that LT represents the only alternative if these therapies fail (28). Although we do not have sufficient experience of PEBD for PFIC1, we now take this anticipatory surgery before LDLT into consideration, if the overall considerations including donor limitations and the patient status indicate the permissive possibility. We understand that PFIC1 patients who eventually have refractory cirrhosis will finally require LT, and we do not consider that PFIC1 contraindicates LDLT because not all of our PFIC1 recipients necessarily suffered graft losses after LDLT. Based on our results, LDLT accompanied by TEBD appears to be rather better than PEBD from the viewpoints of the etiology in PFIC1 and graft protection after LDLT.

Although PFIC1 and PFIC2 share similar laboratory findings, the initial evolution of cholestasis in PFIC2 patients is more severe than in the other PFIC types. Hepatocellular carcinoma may complicate the course. As patients with BSEP deficiency accompanied by biallelic truncating mutations have a considerable risk for hepatobiliary malignancy (15% of patients develop hepatocellular carcinoma or cholangiocarcinoma) (29, 30), close monitoring of malignancy in PFIC2 patients is justified. The histopathological findings reveal more perturbed liver architecture than PFIC1, with more pronounced lobular and portal fibrosis and inflammation. Hepatocellular necrosis and giant cell transformation are also much more pronounced in PFIC2 than in PFIC1. These differences between PFIC1 and PFIC2 probably reflect the severe lobular injury in PFIC2 (4, 9, 10). PFIC2 is caused by mutations in the ABCB11 gene (designated BSEP) (8). The BSEP gene encodes the ATP-dependent canalicular BSEP of the liver and is located on human chromosome 2. The mechanism is shown in Fig. 2C.

PFIC3 can be distinguished from the other types of PFIC because it rarely presents with cholestatic jaundice in the neonatal period, and instead occurs later in infancy and childhood and even in young adulthood. The evolution of the cholestasis is characterized as chronic icteric or anicteric. However, adolescent and young adult patients have cirrhotic symptoms owing to portal hypertension that may result in liver failure. PFIC3 is caused by genetic mutations in the ABCB4 gene (designated MDR3) located on chromosome 7. MDR3 is a phospholipid translocase involved in biliary phospholipid (phosphatidylcholine) excretion and is predominantly expressed in the canalicular membrane of hepatocytes (31). Cholestasis results from toxicity of the bile, in which detergent BSs are not inactivated by phospholipids, thus leading to bile canaliculi and biliary epithelium injuries. A schematic mechanism for PFIC3 is proposed in Fig. 2D.

The mechanism of PFIC1 is still unclear. To our knowledge, the downregulation of cystic fibrosis transmembrane conductance regulator in cholangiocytes has been reported in PFIC1, and this downregulation could contribute to the impairment of bile secretion and explain some of the extrahepatic features (32). The FIC1 gene is expressed in various organs, including the liver, pancreas, small intestine, and kidney, but is more highly expressed in the small intestine than in the liver (33). Therefore, enterohepatic cycling of BS should be considered in PFIC1, and this is a possible explanation of our experiences that PFIC1 recipients easily showed steatosis/steatohepatitis even after LDLT and that PFIC2 recipients showed no steatosis/steatohepatitis after LDLT.

Only one mutated allele or no mutation is rarely identified in a few PFIC patients (< 10%) (1). Mutations that may map to regulatory sequences of the genes are a possible explanation for these findings. A gene involved in the transcription of the PFIC genes (i.e., FXR) or in protein trafficking could also be involved (34, 35). It cannot be negated that other unidentified genes involved in bile formation may be responsible for the PFIC1/2/3 phenotypes. Furthermore, it can be

hypothesized that combined heterozygous mutations for MDR3 and BSEP lead to PFIC-like phenotypes (36). Another possible explanation is that the mutated protein may have a dominant-negative effect on the expression and/or function of the protein in a heterozygous state (37). Modifier genes and environmental influences could play roles in the expression of PFIC (3). The possibility of recurrence of PFIC after LT owing to alloimmunization of the recipient against the FIC1, BSEP or MDR3 proteins of the liver donor remains a theoretical matter of debate (1). It is hypothesized that PFIC patients with a severe mutation leading to the absence of the gene product would be immunologically naive for the FIC1, BSEP or MDR3 gene products. Moreover, alloimmunization necessarily occurs after LT. Although evidence regarding this possible hypothesis after LT has not been reported (28, 38), a case of a PFIC2 patient who experienced an unexplained severe bout of pure hepatocellular cholestasis resembling PFIC2 after deceased-donor LT has been reported (1). In the case of LDLT based on donor relationships with parents, it can be expected that the heterozygous status of the liver allograft leads to a predisposition for developing lithiasis or cholestasis favored by immunosuppressive drugs (39) that may interfere with canalicular protein function, as reported in a PFIC2 patient (1). We consider that this possibility is very rare as there is only one previous report (1), and we performed LDLT in which the donor origins were parents in 10 of 11 recipients (91%) without PFIC recurrences and a previous series of LDLT for PFIC is already documented (38). Our data and a review of the mechanisms by which previous papers have demonstrated that PFIC2 is indicated for LT, including LDLT, as a definitive therapy, similar to other diseases indicated for LT, and also that the clinical courses and outcomes after LDLT are still not sufficient for PFIC1 recipients owing to early post-operative steatosis/fibrosis. Although PFIC1 patients will require LT during the long-term progression of the disease, we suggest that LDLT for PFIC1 may be reconsidered especially with regard to the timing of LDLT under the current donor shortage. Moreover, the establishment of alternative and/or anticipatory strategies for LDLT induction is needed to improve the long-term prognosis of PFIC1.

Acknowledgements

This work was supported by the grants of the Uehara Memorial Foundation (No. 200940051, Tokyo, 171-0033, Japan).

Authors' contributions

T. Hori wrote the paper and performed this research. M. Ueda, F. Oike, Y. Ogura, S. Sakamoto, M. Kasahara, K. Ogawa, Y. Yonekawa, K.I. Watanabe and H. Doi provided important opinions based on their specialized experiences. A. Miyagawa-Hayashino performed histopathological examinations. F. Chen, A.M.T. Baine, and L.B. Gardner helped to perform this research. Prof. S. Uemoto, Prof. Y. Takada, Prof. H. Egawa and Prof. T. Yorifuji designed this research. Prof. S. Uemoto and Prof. J.H. Nguyen supervised this research.

Ethical approval

The protocol of this study was approved by the Ethics Review Committee for Clinical Studies of Kyoto University Graduate School of Medicine.

References

1. Davit-Spraul A, Gonzales E, Baussan C, Jacquemin E. Progressive familial intrahepatic cholestasis. Orphanet J Rare Dis 2009: 4: 1.
2. Jacquemin E, De Vree JM, Cresteil D et al. The wide spectrum of multidrug resistance 3 deficiency: from neonatal cholestasis to cirrhosis of adulthood. Gastroenterology 2001: 120: 1448.
3. Balistreri WF. Inborn errors of bile acid biosynthesis and transport. Novel forms of metabolic liver disease. Gastroenterol Clin North Am 1999: 28: 145.
4. Jacquemin E. Progressive familial intrahepatic cholestasis. Genetic basis and treatment. Clin Liver Dis 2000: 4: 753.
5. Bull LN, Carlton VE, Stricker NL et al. Genetic and morphological findings in progressive familial intrahepatic cholestasis (Byler disease [PFIC-1] and Byler syndrome): evidence for heterogeneity. Hepatology 1997: 26: 155.
6. Jansen PL, Strautnieks SS, Jacquemin E et al. Hepatocanalicular bile salt export pump deficiency in patients with progressive familial intrahepatic cholestasis. Gastroenterology 1999: 117: 1370.
7. van Mil SW, Klomp LW, Bull LN, Houwen RH. FIC1 disease: a spectrum of intrahepatic cholestatic disorders. Semin Liver Dis 2001: 21: 535.
8. Thompson R, Strautnieks S. BSEP: function and role in progressive familial intrahepatic cholestasis. Semin Liver Dis 2001: 21: 545.
9. Chen HL, Chang PS, Hsu HC et al. FIC1 and BSEP defects in Taiwanese patients with chronic intrahepatic cholestasis with low gamma-glutamyltranspeptidase levels. J Pediatr 2002: 140: 119.
10. Lykavieris P, van Mil S, Cresteil D et al. Progressive familial intrahepatic cholestasis type 1 and extrahepatic features: no catch-up of stature growth, exacerbation of diarrhea, and appearance of liver steatosis after liver transplantation. J Hepatol 2003: 39: 447.
11. Jacquemin E, Hermans D, Myara A et al. Ursodeoxycholic acid therapy in pediatric patients with progressive familial intrahepatic cholestasis. Hepatology 1997: 25: 519.

12. Ganne-Carrie N, Baussan C, Grando V, Gaudelus J, Cresteil D, Jacquemin E. Progressive familial intrahepatic cholestasis type 3 revealed by oral contraceptive pills. J Hepatol 2003: 38: 693.
13. Hayashi H, Sugiyama Y. 4-phenylbutyrate enhances the cell surface expression and the transport capacity of wild-type and mutated bile salt export pumps. Hepatology 2007: 45: 1506.
14. Balistreri WF, Bezerra JA, Jansen P, Karpen SJ, Shneider BL, Suchy FJ. Intrahepatic cholestasis: summary of an American Association for the Study of Liver Diseases single-topic conference. Hepatology 2005: 42: 222.
15. De Vree JM, Ottenhoff R, Bosma PJ, Smith AJ, Aten J, Oude Elferink RP. Correction of liver disease by hepatocyte transplantation in a mouse model of progressive familial intrahepatic cholestasis. Gastroenterology 2000: 119: 1720.
16. Boyer JL. Nuclear receptor ligands: rational and effective therapy for chronic cholestatic liver disease? Gastroenterology 2005: 129: 735.
17. Egawa H, Teramukai S, Haga H et al. Present status of ABO-incompatible living donor liver transplantation in Japan. Hepatology 2008: 47: 143.
18. Miyagawa-Hayashino A, Egawa H, Yorifuji T et al. Allograft steatohepatitis in progressive familial intrahepatic cholestasis type 1 after living donor liver transplantation. Liver Transpl 2009: 15: 610.
19. Brunt EM. Nonalcoholic steatohepatitis: definition and pathology. Semin Liver Dis 2001: 21: 3.
20. Intraobserver and interobserver variations in liver biopsy interpretation in patients with chronic hepatitis C. The French METAVIR Cooperative Study Group. Hepatology 1994: 20: 15.
21. Chen F, Ananthanarayanan M, Emre S et al. Progressive familial intrahepatic cholestasis, type 1, is associated with decreased farnesoid X receptor activity. Gastroenterology 2004: 126: 756.
22. Bassas A, Chehab M, Hebby H et al. Living related liver transplantation in 13 cases of progressive familial intrahepatic cholestasis. Transplant Proc 2003: 35: 3003.
23. Arnell H, Bergdahl S, Papadogiannakis N, Nemeth A, Fischler B. Preoperative observations and short-term outcome after partial external biliary diversion in 13 patients with progressive familial intrahepatic cholestasis. J Pediatr Surg 2008: 43: 1312.
24. Kalicinski PJ, Ismail H, Jankowska I et al. Surgical treatment of progressive familial intrahepatic cholestasis: comparison of partial external biliary diversion and ileal bypass. Eur J Pediatr Surg 2003: 13: 307.
25. Modi BP, Suh MY, Jonas MM, Lillehei C, Kim HB. Ileal exclusion for refractory symptomatic cholestasis in Alagille syndrome. J Pediatr Surg 2007: 42: 800.
26. Bustorff-Silva J, Sbraggia Neto L, Olimpio H et al. Partial internal biliary diversion through a cholecystojejunocolonic anastomosis–a novel surgical approach for patients with progressive familial intrahepatic cholestasis: a preliminary report. J Pediatr Surg 2007: 42: 1337.
27. Stapelbroek JM, van Erpecum KJ, Klomp LW et al. Nasobiliary drainage induces long-lasting remission in benign recurrent intrahepatic cholestasis. Hepatology 2006: 43: 51.
28. Soubrane O, Gauthier F, DeVictor D et al. Orthotopic liver transplantation for Byler disease. Transplantation 1990: 50: 804.
29. Strautnieks SS, Byrne JA, Pawlikowska L et al. Severe bile salt export pump deficiency: 82 different ABCB11 mutations in 109 families. Gastroenterology 2008: 134: 1203.
30. Knisely AS, Strautnieks SS, Meier Y et al. Hepatocellular carcinoma in ten children under five years of age with bile salt export pump deficiency. Hepatology 2006: 44: 478.
31. Jacquemin E. Role of multidrug resistance 3 deficiency in pediatric and adult liver disease: one gene for three diseases. Semin Liver Dis 2001: 21: 551.
32. Demeilliers C, Jacquemin E, Barbu V et al. Altered hepatobiliary gene expressions in PFIC1: ATP8B1 gene defect is associated with CFTR downregulation. Hepatology 2006: 43: 1125.
33. Bull LN, van Eijk MJ, Pawlikowska L et al. A gene encoding a P-type ATPase mutated in two forms of hereditary cholestasis. Nat Genet 1998: 18: 219.
34. Van Mil SW, Milona A, Dixon PH et al. Functional variants of the central bile acid sensor FXR identified in intrahepatic cholestasis of pregnancy. Gastroenterology 2007: 133: 507.
35. Paulusma CC, Folmer DE, Ho-Mok KS et al. ATP8B1 requires an accessory protein for endoplasmic reticulum exit and plasma membrane lipid flippase activity. Hepatology 2008: 47: 268.
36. Rosmorduc O, Hermelin B, Poupon R. MDR3 gene defect in adults with symptomatic intrahepatic and gallbladder cholesterol cholelithiasis. Gastroenterology 2001: 120: 1459.
37. Ortiz D, Arias IM. MDR3 mutations: a glimpse into pandora's box and the future of canalicular pathophysiology. Gastroenterology 2001: 120: 1549.
38. Cutillo L, Najimi M, Smets F et al. Safety of living-related liver transplantation for progressive familial intrahepatic cholestasis. Pediatr Transplant 2006: 10: 570.
39. Pauli-Magnus C, Meier PJ. Hepatobiliary transporters and drug-induced cholestasis. Hepatology 2006: 44: 778.

CLINICAL GENETICS An International Journal of Genetics, Molecular and Personalized Medicine

Clin Genet 2011: 80: 478–483
Printed in Singapore. All rights reserved

CLINICAL GENETICS
doi: 10.1111/j.1399-0004.2010.01599.x

Short Report

Maternal uniparental isodisomy and heterodisomy on chromosome 6 encompassing a *CUL7* gene mutation causing 3M syndrome

Sasaki K, Okamoto N, Kosaki K, Yorifuji T, Shimokawa O, Mishima H, Yoshiura K-i, Harada N. Maternal uniparental isodisomy and heterodisomy on chromosome 6 encompassing a *CUL7* gene mutation causing 3M syndrome.
Clin Genet 2011: 80: 478–483. © John Wiley & Sons A/S, 2010

We report a case of segmental uniparental maternal hetero- and isodisomy involving the whole of chromosome 6 (mat-hUPD6 and mat-iUPD6) and a cullin 7 (*CUL7*) gene mutation in a Japanese patient with 3M syndrome. 3M syndrome is a rare autosomal recessive disorder characterized by severe pre- and postnatal growth retardation that was recently reported to involve mutations in the *CUL7* or obscurin-like 1 (*OBSL1*) genes. We encountered a patient with severe growth retardation, an inverted triangular gloomy face, an inverted triangle-shaped head, slender long bones, inguinal hernia, hydrocele testis, mild ventricular enlargement, and mild mental retardation. Sequence analysis of the *CUL7* gene of the patient revealed a homozygous missense mutation, c.2975G>C. Genotype analysis using a single nucleotide polymorphism array revealed two mat-hUPD and two mat-iUPD regions involving the whole of chromosome 6 and encompassing *CUL7*. 3M syndrome caused by complete paternal iUPD of chromosome 6 involving a *CUL7* mutation has been reported, but there have been no reports describing 3M syndrome with maternal UPD of chromosome 6. Our results represent a combination of iUPDs and hUPDs from maternal chromosome 6 involving a *CUL7* mutation causing 3M syndrome.

Conflict of interest

None of the authors of this paper declares a conflict of interest.

K Sasaki[a], N Okamoto[b], K Kosaki[c], T Yorifuji[d], O Shimokawa[e], H Mishima[a], K-i Yoshiura[a] and N Harada[e]

[a]Department of Human Genetics, Nagasaki University Graduate School of Biomedical Sciences, Nagasaki, Japan, [b]Osaka Medical Center and Research Institute for Maternal and Child Health, Osaka, Japan, [c]Department of Pediatrics, Keio University School of Medicine, Tokyo, Japan, [d]Department of Pediatric Endocrinology and Metabolism, Children's Medical Center, Osaka City General Hospital, Osaka, Japan, and [e]Cytogenetic Testing Group B, Advanced Medical Science Research Center, Mitsubishi Chemical Medience Corporation, Nagasaki, Japan

Key words: 3M syndrome – cullin 7 (*CUL7*) – Genome-Wide Human SNP Array 6.0 (SNP6.0) – maternal uniparental disomy of chromosome 6 (matUPD6)

Corresponding author: Dr Koh-ichio Yoshiura, Department of Human Genetics, Nagasaki University Graduate School of Biomedical Sciences, Sakamoto 1-12-4, Nagasaki 852-8523, Japan.
Tel.: +81 95 819 7118;
fax: +81 95 849 7121;
e-mail: kyoshi@nagasaki-u.ac.jp

Received 10 September 2010, revised and accepted for publication 12 November 2010

3M syndrome is a rare inherited autosomal recessive disorder characterized by pre- and postnatal growth retardation, characteristic facial features, and skeletal anomalies. Clinical features of 3M syndrome include large head circumference, broad forehead, a triangular facial outline, dolichocephaly, long philtrum, short stature, short thorax and neck, tall vertebral bodies, and slender

long bones and ribs. Males with 3M syndrome occasionally have hypogonadism and hypospadias (1–9). However, intelligence is unaffected and karyotype is normal on conventional chromosome analysis.

In patients with 3M syndrome, disease-causing mutations have been identified in the cullin 7 (*CUL7*, MIM *609577) and obscurin-like 1 (*OBSL1*, MIM *610991) genes (7–9). Mutations of *CUL7* are the major cause of 3M syndrome, accounting for 80% of previously reported cases, whereas *OBSL1* accounts for 20% of cases (8, 10).

Uniparental disomy (UPD) is the transmission pattern of either two copies of the identical chromosome (uniparental isodisomy; iUPD) or of both homologous chromosomes (uniparental heterodisomy; hUPD) from one parent with no contribution from the other parent (11). Phenotypes that are clinically associated with paternal UPD of chromosome 6 (patUPD6) and genomic imprinting have been established, but because of the rarity of maternal UPD of chromosome 6 (matUPD6), clinical features have not yet been established. Here, we report a patient with a homozygous mutation in *CUL7* due to a maternal iUPD of chromosome 6 (mat-iUPD6).

Materials and methods

Clinical report

A Japanese male patient with 3M syndrome was examined in this study. The patient was delivered by caesarean section at 36 weeks of gestation without a family history of 3M syndrome (Fig. 1a). His birth weight was 1000 g (−4.8 SD), length 33.0 cm (−6.8 SD), head circumference 30.2 cm (−1.5 SD), and Apgar score 7/9. Feeding difficulty was noted during the neonatal period. He remained in a neonatal intensive care unit for 2 months and was referred to our group because of developmental delay and muscle hypotonia at 4 months. The patient displayed anomalies including hypospadias, inguinal hernia, hydrocele testis, inverted triangular gloomy face, malar hypoplasia, long eyelashes, epicanthal folds, short nose, anteverted nares, full lips, long philtrum, pointed chin, short chest, grooved lower anterior thorax, hypermobility of joints, and slender long bones (Fig. 1a,b). Mild ventricular enlargement was observed by neuroradiological studies. His growth was severely retarded.

At 2 years 9 months, his height, weight, and head circumference were 69.3 cm (−4.6 SD), 6.8 kg (−6.7 SD), and 48 cm (−1.2 SD), respectively. His head size was disproportionately large compared to his height. Thus the patient was diagnosed as suffering from 3M syndrome. He could understand simple sentences, but could not speak nor sit alone. Partial growth hormone (GH) deficiency was noted. GH replacement therapy was started from 2 years. GH was effective without side effects. At 5 years, his height and weight were 84.8 cm (−5.9 SD) and 10 kg (−3 SD), respectively. He was moderately mentally retarded.

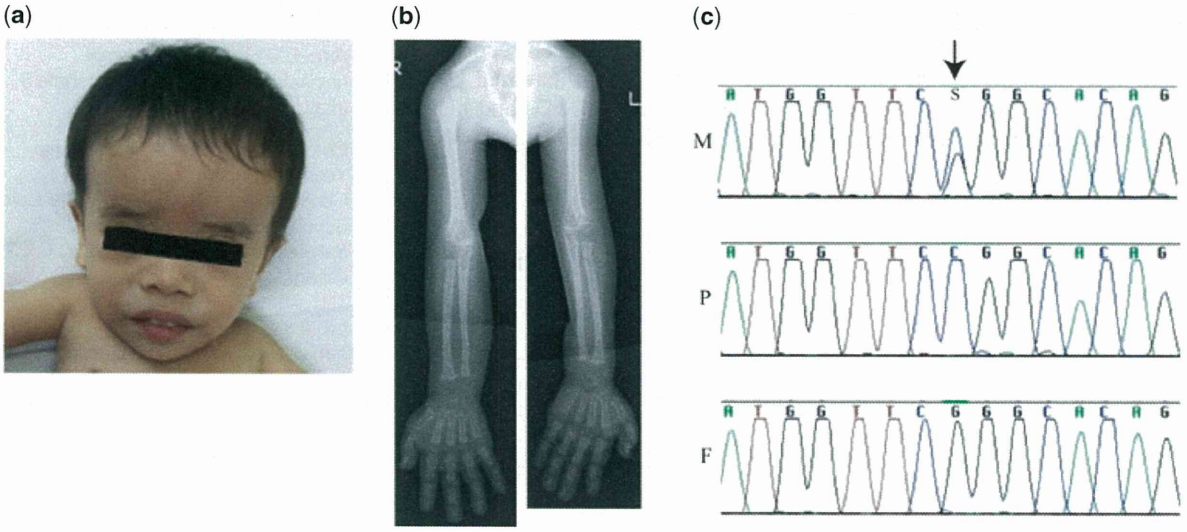

Fig. 1. Facial and skeletal features of the patient at 2 years 7 months of age. (**a**) Note the inverted triangular gloomy face, short nose, full lips, and long philtrum. (**b**) Note the slender long bones. (**c**) Electropherograms of the patient and parents. DNA sequence showing a single base change substituting cytosine for guanine, which results in p.R992P, in the patient. M, mother; P, patient; and F, father.

Conventional cytogenetic studies and FISH analysis

We obtained blood samples under written informed consent for participation in this study. Conventional cytogenetic examination of G-banded chromosomes from peripheral blood lymphocytes was performed. We also performed fluorescence *in situ* hybridization (FISH) analysis on lymphocyte metaphase spreads from the patient using two Bacterial Artificial Chromosome (BAC) clones containing *CUL7*, RP11-628J2 and RP11-653G5, as probes.

Genomic sequencing

Genomic DNA was extracted from peripheral blood following standard protocols. For mutation analysis, we designed primers to amplify all the coding exons of *CUL7* and the flanking intron sequences. Direct sequencing was carried out using a BigDye Terminator v3.1 Cycle sequencing Kit™ and separated on a Genetic Analyzer 3130*xl* (Applied Biosystems Inc., Foster City, CA). Sequence electropherograms were aligned with SEQUENCHER™ software (Gendcodes, Ann Arbor, MI) to visually inspect base alterations.

Microarray analysis

We performed genome-wide single nucleotide polymorphism (SNP) genotyping using Genome-Wide Human SNP Array 6.0 (SNP6.0) following the manufacturer's instructions (Affymetrix, Santa Clara, CA, http://www.affymetrix.com/index.affx). The data generated from Genotyping Console (GTC) 4.0 were loaded into CHROMOSOME ANALYSIS SUITE (CHAS) 1.0.1 software to display the results. We carried out UPD analyses of the patient using genotype data in trio. Genomic positions of SNPs corresponded to the March 2006 human genome (hg18).

Results

Genomic sequencing

We sequenced all 26 coding exons and flanking intronic regions of the *CUL7* gene, which spans a genomic region of approximately 16.3 kb, in the family. In the patient, we detected a homozygous missense mutation (c.2975G>C) in exon 15, which resulted in the substitution of proline for arginine at amino acid residue 992 (p.R992P) (Fig. 1c). The mother was a heterozygous carrier of the mutation, whereas the father was homozygous for the wild-type allele (Fig. 1c). The p.R992P mutation was not detected in 100 unrelated control individuals.

Conventional and molecular cytogenetic analyses

G-banding and FISH analysis at the *CUL7* locus showed a normal karyotype in the patient and the parents with no microdeletion at *CUL7* locus in the patient (data not shown).

Microarray analysis

To confirm paternity, and to find a small size deletion, we performed SNP6.0 analysis. However, no copy number variations (CNVs) were identified in the region containing both *CUL7* and *OBSL1* genes (Fig. 2a). The other variants overlap with reported regions of CNVs in the Database of Genomic Variants (http://projects.tcag.ca/variation) or were transmitted from the parents (data not shown).

To confirm matUPD6 in the patient, we examined the genotypes of the patient/father/mother trio. The results using informative markers indicated that there were two maternal heterodisomic regions (hUPD6-1 and hUPD6-2) and two maternal isodisomic regions (iUDP6-1 and iUPD6-2) in chromosome 6, respectively (Fig. 2 and Table 1). The results indicated that the patient had inherited two alleles from his mother, but none from his father, in chromosome 6. The final karyotype of this patient was 46,XY,upd(6)mat and arr 6p25.3p22.3(110,391–16,287,166)×2 htz mat,6p 22.3q12(16,290,223–65,796,893)×2 hmz mat,6q 12q25.1(65,799,990–150,517,779)×2 htz mat,6q 25.1q27(150,518,012–170,759,956)×2 hmz mat.

Discussion

We identified a causative homozygous mutation in *CUL7* in a patient with 3M syndrome. The results clearly indicate that mat-iUPD6 involving a mutant allele of the *CUL7* gene caused 3M syndrome in the patient.

matUPD6 is relatively rare and seven cases have been reported. The first case was a renal transplant patient who showed growth retardation at birth and mat-iUPD6 (12). The second case was a patient with congenital adrenal hyperplasia (CAH) resulting from a homozygous mutation in the 21-hydroxylase gene (*CYP21*), and had intrauterine growth retardation (IUGR) and mat-iUPD6 (13). The third case was a macerated male fetus from a pregnancy terminated at 23 weeks of gestation because of intrauterine death. The patient showed a mosaic trisomy 6 (14). The fourth case was a male patient with two clinical phenotypes, Klinefelter's syndrome and CAH. His karyotype was mosaic 48,XXY, +mar[30]/47,XXY[20] and

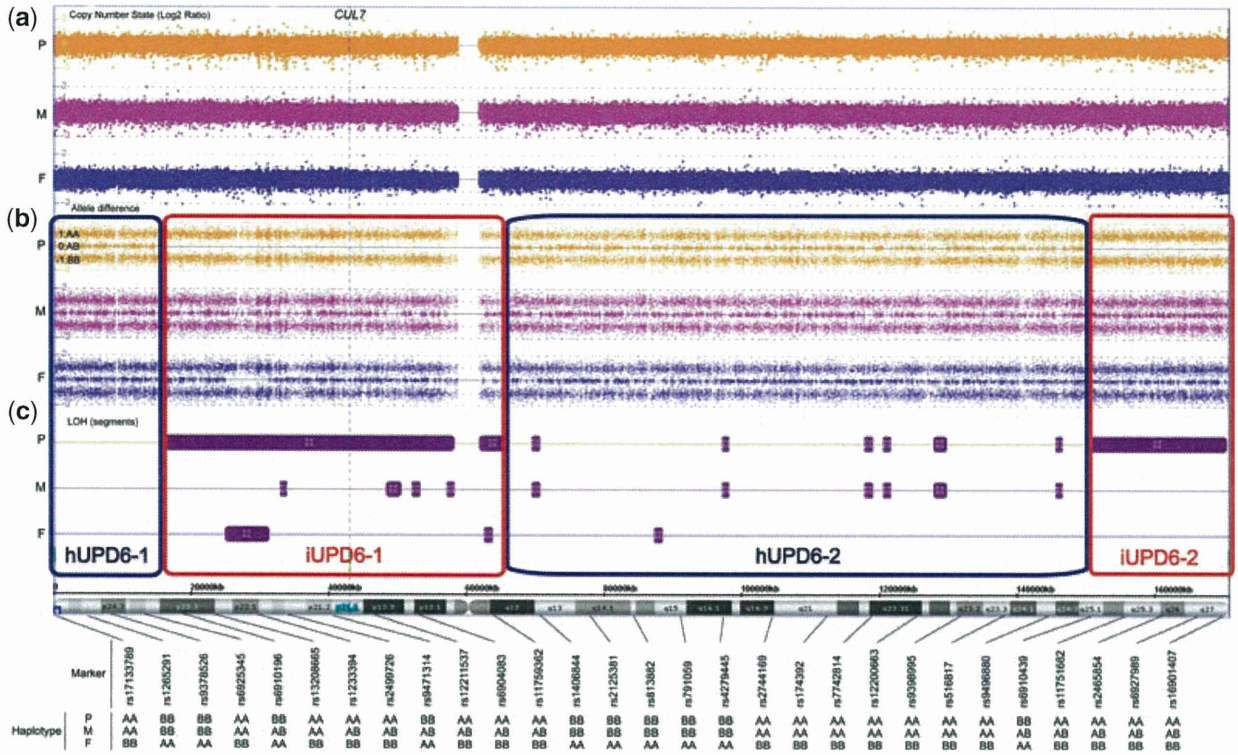

Fig. 2. SNP6.0 data. (**a**) Plots of the SNP6.0 data displayed in ChAS 1.0.1 showing the log2 ratio plot of copy number state, allele difference plot, and loss of heterozygosity (LOH) segment (purple box) (P, patient; M, mother; and F, father). (**b**) The allele difference graph represents the genotypes for each individual single nucleotide polymorphism (SNP). Dots with a value of 1, −1, and 0 represent SNPs with AA, BB, and AB genotypes, respectively. A vertical dashed line indicates the *CUL7* locus. (**c**) The LOH segment plot indicates nine LOH regions on chromosome 6. iUPD6-1 and iUPD6-2 denote the regions of uniparental isodisomy (red box). hUPD6-1 and hUPD6-2 denote the regions of uniparental heterodisomy (blue box). The genotypes on chromosome 6 indicate maternal heterodisomy or isodisomy in the affected offspring [only the uniparental disomy (UPD) markers are displayed].

Table 1. Examination of SNPs from a patient/father/mother trio[a]

			hUPD6-1	iUPD6-1	hUPD6-2	iUPD6-2
Genotype of trio (patient/father/mother)	iUPD	AA/BB/AB	0	534	0	318
		BB/AA/AB	0	576	3	304
	iUPD or hUPD	AA/BB/AA	178	543	605	272
		BB/AA/BB	196	506	563	262
Share genotype (patient/mother)	iUPD or hUPD	AA/AA	2,812	5,897	9,716	3,009
		BB/BB	2,799	5,785	9,557	2,919
	hUPD	AB/AB	1,699	19	6,384	12
		Total of share genotype	7,310	11,701	25,657	5,940
		Share genotype rate (%)	99.82	78.20	99.89	73.31
		Total SNP probe	7,323	14,963	25,684	8,103
		Start SNP	rs4959515	rs9370869	rs9354209	rs9384189
		Start position	110,391	16,290,223	65,799,990	150,518,012
		End SNP	rs9477050	rs9453156	rs7765984	rs6931065
		End position	16,287,166	65,796,893	150,517,779	170,759,956
		Size (bp)	16,176,776	49,506,671	84,717,790	20,241,945
		Cytoband	p25.3-p22.3	p22.3-q12	q12-q25.1	q25.1-q27

hUPD, uniparental heterodisomy; iUPD, uniparental isodisomy; iUPD or hUPD, UPD could not be defined as isodisomy or heterodisomy; SNP, single nucleotide polymorphism.

[a]Each row contains information on each matUPD6 inheritance block identified by trio haplotype analysis.

both the X chromosome and chromosome 6 showed maternal iUPD. This case also was notable for IUGR and growth retardation at 8 months of age (15). The fifth case was a fetus with IUGR at 29 weeks of pregnancy from a 45-year-old patient. The case was ascertained as trisomy 6 mosaicism in cultured chorionic villi but disomy in amniocytes; analysis of DNA markers in amniocytes and parental samples revealed mat-iUPD6 in disomy cells (16). The sixth case was a male infant with molybdenum cofactor deficiency who showed developmental delay. SNP analysis with the trio revealed that at least 6p21.1-6p24.3 were mat-iUPD6, but not another region were remain unclear (17). The seventh case was a patient with cleft lip and palate, and showed a complete maternal hUPD on chromosome 6 (mat-hUPD6). This case had no notable IUGR in the serial ultrasound examination (18). Taken together, IUGR and growth retardation were found in the cases with mat-iUPD6 (12, 13, 15–17), while these were not found in cases with mat-hUPD6 (14, 18). The IUGR and growth retardation in cases of mat-iUPD6 may be the result of homozygosity of chromosome 6. On the basis of these reports, no clear maternal imprinting effect of chromosome 6 can be established; however, recently, a complete gain of methylation phenotype at insulin-like growth factor 2 receptor was shown in patients with growth restriction (19).

The patient with homozygous mutation in *CUL7* and matUPD6 had clinical features compatible with 3M syndrome. However, the patient displayed certain features that have not been previously reported among patients with *CUL7* mutations such as mild mental retardation, inguinal hernia, hydrocele testis, and mild ventricular enlargement (7, 8, 20). Mild mental retardation is an especially characteristic phenotype in our case because most patients with 3M syndrome have normal intelligence. It is difficult to determine whether matUPD6 had a significant role in the development of certain feature in our case.

Here we report a case of 3M syndrome with a homozygous mutation that resulted from maternal iUPD, including the *CUL7* gene. Although complete paternal or maternal UPD for chromosome 6 has previously been reported, this is the first report of a patient with 3M syndrome who has a mixture of mat-hUPD6 and mat-iUPD6 regions. Our results emphasize that UPD should be considered possible mechanism for developing the autosomal recessive disorders including 3M syndrome.

Acknowledgements

We are grateful to the patient and his parents for their participation in this research. We also thank Ms Miho Ooga and Ms Chisa Hayashida for technical assistance. K.-I. Y. was supported in part by Grants-in-Aid for Scientific Research from the Ministry of Health, Labour and Welfare, and in part by the Takeda Scientific Foundation and the Naito Foundation.

References

1. Winter RM, Baraitser M, Grant DB, Preece MA, Hall CM. The 3-M syndrome. J Med Genet 1984: 21: 124–128.
2. Feldmann M, Gilgenkrantz S, Parisot S, Zarini G, Marchal C. 3M dwarfism: a study of two further sibs. J Med Genet 1989: 26 (9): 583–585.
3. García-Cruz D, Cantú JM. Heterozygous expression in 3-M slender-boned nanism. Hum Genet 1979: 52: 221–226.
4. Mueller RF, Buckler J, Arthur R et al. The 3-M syndrome: risk of intracerebral aneurysm? J Med Genet 1992: 29: 425–427.
5. Le Merrer M, Brauner R, Maroteaux P. Dwarfism with gloomy face: a new syndrome with features of 3-M syndrome. J Med Genet 1991: 28: 186–191.
6. Spranger J, Opitz JM, Nourmand A. A new familial intrauterine growth retardation syndrome the "3-M syndrome". Eur J Pediatr 1976: 123: 115–124.
7. Huber C, Dias-Santagata D, Glaser A et al. Identification of mutations in *CUL7* in 3-M syndrome. Nat Genet 2005: 37: 1119–1124.
8. Huber C, Delezoide AL, Guimiot F et al. A large-scale mutation search reveals genetic heterogeneity in 3M syndrome. Eur J Hum Genet 2009: 17: 395–400.
9. Hanson D, Murray PG, Sud A et al. The primordial growth disorder 3-M syndrome connects ubiquitination to the cytoskeletal adaptor *OBSL1*. Am J Hum Genet 2009: 84: 801–806.
10. Huber C, Fradin M, Edouard T et al. OBSL1 mutations in 3-M syndrome are associated with a modulation of IGFBP2 and IGFBP5 expression levels. Hum Mutat 2010: 31: 20–26.
11. Engel E. A new genetic concept: uniparental disomy and its potential effect, isodisomy. Am J Med Genet 1980: 6: 137–143.
12. van den Berg-Loonen EM, Savelkoul P, van Hooff H, van Eede P, Riesewijk A, Geraedts J. Uniparental maternal disomy 6 in a renal transplant patient. Hum Immunol 1996: 45: 46–51.
13. Spiro RP, Christian SL, Ledbetter DH et al. Intrauterine growth retardation associated with maternal uniparental disomy for chromosome 6 unmasked by congenital adrenal hyperplasia. Pediatr Res 1999: 46: 510–513.
14. Cockwell AE, Baker SJ, Connarty M, Moore IE, Crolla JA. Mosaic trisomy 6 and maternal uniparental disomy 6 in a 23-week gestation fetus with atrioventricular septal defect. Am J Med Genet A 2006: 140: 624–627.
15. Parker EA, Hovanes K, Germak J, Porter F, Merke DP. Maternal 21-hydroxylase deficiency and uniparental isodisomy of chromosome 6 and X results in a child with 21-hydroxylase deficiency and Klinefelter syndrome. Am J Med Genet A 2006: 140: 2236–2240.
16. Haag M, Beischel L, Rokeach J et al. First prenatal detection of maternal uniparental disomy (UPD) of chromosome 6 and 'rescue' of trisomy 6 [abstract]. *Abstracts of the 57th Annual Meeting of the ASHG 2007*; Abstract no 2428.
17. Gümüş H, Ghesquiere S, Per H et al. Maternal uniparental isodisomy is responsible for serious molybdenum cofactor deficiency. Dev Med Child Neurol 2010: 52 (9): 868–872.

18. Salahshourifar I, Halim AS, Sulaiman WA, Zilfalil BA. Maternal uniparental heterodisomy of chromosome 6 in a boy with an isolated cleft lip and palate. Am J Med Genet A 2010: 152A (7): 1818–1821.
19. Turner CL, Mackay DM, Callaway JL et al. Methylation analysis of 79 patients with growth restriction reveals novelpatterns of methylation change at imprinted loci. Eur J Hum Genet 2010: 18: 648–655.
20. Maksimova N, Hara K, Miyashia A et al. Clinical, molecular and histopathological features of short stature syndrome with novel *CUL7* mutation in Yakuts: new population isolate in Asia. J Med Genet 2007: 44: 772–778.

Brief Report—Endocrine Research

Molecular and Clinical Analysis of Japanese Patients with Persistent Congenital Hyperinsulinism: Predominance of Paternally Inherited Monoallelic Mutations in the K_{ATP} Channel Genes

Tohru Yorifuji, Rie Kawakita, Shizuyo Nagai, Akinori Sugimine, Hiraku Doi, Anryu Nomura, Michiya Masue, Hironori Nishibori, Akihiko Yoshizawa, Shinya Okamoto, Ryuichiro Doi, Shinji Uemoto, and Hironori Nagasaka

Department of Pediatric Endocrinology and Metabolism (T.Y.), Osaka City General Hospital, Osaka 543-0021, Japan; Departments of Pediatrics (T.Y., R.K., S.N., A.S., H.D., A.N.), Diagnostic Pathology (A.Y.), and Surgery (S.O., R.D., S.U.), Kyoto University Hospital, Kyoto 606-8507, Japan; Departments of Pediatrics (M.M.) and Radiology (H.N.), Kizawa Memorial Hospital, Gifu 505-8503, Japan; Department of Pediatrics (H.N.), Takarazuka City Hospital, Takarazuka 665-0827, Japan

Background: Preoperative identification of the focal form of congenital hyperinsulinism is important for avoiding unnecessary subtotal pancreatectomy. However, neither the incidence nor the histological spectrum of the disease is known for Japanese patients.

Aims: The aim of the study was to elucidate the molecular and histological spectrum of congenital hyperinsulinism in Japan.

Subjects: Thirty-six Japanese infants with persistent congenital hyperinsulinism were included in the study.

Methods: All exons of the ATP-sensitive potassium channel (K_{ATP} channel) genes (*KCNJ11* and *ABCC8*), the *GCK* gene, and exons 6 and 7 and 10–12 of the *GLUD1* gene were amplified from genomic DNA and directly sequenced. In patients with K_{ATP} channel mutations, the parental origin of each mutation was determined, and the results were compared with the histological findings of surgically treated patients. In one of the patients with scattered lesions, islets were sampled by laser capture microdissection for mutational analysis.

Results: Mutations were identified in 24 patients (66.7%): five in *GLUD1* and 19 in the K_{ATP} channel genes. Sixteen had a paternally derived, monoallelic K_{ATP} channel mutation predictive of the focal form. In 10 patients who underwent pancreatectomy, the molecular diagnosis correctly predicted the histology, more accurately than [18F]-3,4-dihydroxyphenylalanine positron emission tomography scans. Three patients showed focal lesions that occupied larger areas of the pancreas. Preferential loss of the maternal allele was observed in these islets.

Conclusion: The majority of the Japanese patients with K_{ATP} channel hyperinsulinism (84.2%) demonstrated paternally inherited monoallelic mutations that accurately predicted the presence of the focal form. **(*J Clin Endocrinol Metab* 96: E141–E145, 2011)**

Persistent congenital hyperinsulinism is the main cause of prolonged hypoglycemia in infancy. The most common etiology is an inactivating mutation in one of two genes, *ABCC8* or *KCNJ11*, which code for the two subunits of the pancreatic ATP-sensitive potassium (K_{ATP}) channel. The second most common is an activating mu-

ISSN Print 0021-972X ISSN Online 1945-7197
Printed in U.S.A.

doi: 10.1210/jc.2010-1281 Received June 7, 2010. Accepted September 16, 2010.
First Published Online October 13, 2010

Abbreviations: DOPA, 3,4-Dihydroxyphenylalanine; GCK, glucokinase; GLUD1, glutamate dehydrogenase; K_{ATP}, ATP-sensitive potassium channel; MLPA, multiple ligation-dependent probe amplification; PET, positron emission tomography.

tation in the glutamate dehydrogenase (*GLUD1*) gene, which is found in cases of hyperinsulinemia-hyperammonemia syndrome followed by an activating mutation in the glucokinase (*GCK*) gene with a much rare incidence (1).

Because severely affected infants often experience profound neurological sequelae (2, 3), appropriate management of hypoglycemia is critically important. Infants resistant to medical treatment usually undergo subtotal pancreatectomy. Although the procedure is often effective at controlling hypoglycemia, residual hypoglycemia is not uncommon, and many of the infants develop insulin-dependent diabetes mellitus postoperatively (1, 4).

Notably, the recognition of the focal form of persistent congenital hyperinsulinism has changed clinical practice because precise pre- and intraoperative identification of focal lesions allows us to perform a partial resection of the pancreas, leading to a complication-free cure (1, 5, 6).

Focal lesions are found in individuals with a paternally inherited, monoallelic K_{ATP} channel mutation (5–7). Subsequent somatic loss of the maternal allele (most likely caused by paternal isodisomy) leads to a loss of the activities of the K_{ATP} channel and the adjacent tumor suppressors (*H19* and *CDKN1C*) normally expressed by the maternal allele. These cells gain a growth advantage eventually forming a focal lesion of insulin-overproducing β-cells (8).

It has been reported that approximately 40% of patients with K_{ATP} channel hyperinsulinism have monoallelic mutations (9, 10) and that up to 40–60% of surgically treated patients have the focal form (1, 6, 7). However, to date, neither the incidence of focal lesions nor the clinical spectrum of persistent congenital hyperinsulinism has been reported for Asians.

In this study, we performed a comprehensive mutational analysis of Japanese patients with this disorder and correlated the results with the histology of surgically treated patients.

Subjects and Methods

Subjects

The study subjects were 36 Japanese infants with persistent congenital hyperinsulinism. The inclusion criteria were as follows: 1) a plasma insulin level of greater than 3 μU/ml in the presence of hypoglycemia [plasma glucose < 45 mg/dl (2.5 mmol/liter)], 2) hypoglycemia lasting beyond 3 months of age, and 3) the absence of insulinoma. The patients were born in 2005–2010 except for those with hyperinsulinemia-hyperammonemia syndrome who were recruited over a longer period (born in 1999–2009). For mutational analysis, written informed consent was obtained, and the study protocol was approved by the institutional review board.

Mutational analysis

Genomic DNA was extracted from peripheral blood leukocytes using a QIAmp DNA blood kit (QIAGEN, Hilden, Germany) as recommended by the supplier. Then all exons and the exon-intron boundaries of the *KCNJ11*, *ABCC8*, and *GCK* genes were amplified from genomic DNA. For the *GLUD1* gene, only exons 6 and 7 (the antenna domain) and exons 10–12 (the GTP binding domain) were amplified because previously reported mutations were exclusively found in these regions. The amplification conditions and the sequences of the primers are available as supplemental data, published on The Endocrine Society's Journals Online web site at http://jcem.endojournals.org. The amplified products were purified using the Wizard PCR Preps DNA purification system (Promega, Fitchburg, WI) and directly sequenced using the BigDye Terminator cycle sequencing kit (version 3.1; Applied Biosystems, Foster City, CA).

Deletion mutations that might not have been detected by the PCR-sequencing strategy described above were analyzed by multiple ligation-dependent probe amplification (MLPA) of all 39 exons of the *ABCC8* gene. The analyses were performed using SALSA MLPA kit P117 (MRC Holland, Amsterdam, The Netherlands) as recommended by the manufacturer.

[18F]-3,4-dihydroxyphenylalanine (DOPA) positron emission tomography (PET)

[18F]-DOPA PET studies were performed at the PET facility of Kizawa Memorial Hospital basically, as described by Ribeiro *et al.* (11). The scan results were fused with those of a computed tomography scan taken at the same time to localize the focal lesion more accurately.

Laser capture microdissection (LCM)

The scattered islets of patient 10 were sampled by LCM using the PixCell IIe LCM system (Arcturus, Mountain View, CA). DNA was extracted from the pooled islets using a FASTPURE DNA kit (Takara-bio, Ohtsu, Japan). DNA extracted from a normal pancreatic area on the same slide was used as the control.

Results

Patient profiles and mutations

The profiles of the patients and the results of the mutational analyses are listed in Table 1. In patients with elevated ammonia at the initial presentation, only patients 1–5 showed persistent hyperammonemia. Those five had mutations in *GLUD1*. Of the remaining 31 patients, mutations were identified in 19 (61.3%): 18 in *ABCC8*, one in *KCNJ11*, and none in *GCK*. No exonic deletions were identified by MLPA, and the four novel missense mutations were not found in 100 normal controls. p.R836X and p.R998X in *ABCC8* were identified in five and three unrelated patients, respectively, possibly representing relatively common mutations in Japanese.

Interestingly, of these patients with K_{ATP} channel mutations, only two had biallelic mutations, whereas the

TABLE 1. Profiles of the patients with mutations

Patient no.	Gender	Onset	Glucose (mg/dl) [mmol/liter]	Insulin (μU/ml) [pmol/liter]	Ammonia (μg/dl) [μmol/liter]	Mutation					Medical treatment
						Gene	cDNA	Protein	Previously reported?	Parental origin	
1	F	9 months	38 [2.1]	4.8 [33]	83 [49]	*GLUD1*	c.661C>T	p.R221C	yes	ND	F, D
2	M	7 months	30 [1.7]	3 [21]	132 [77]	*GLUD1*	c.797A>G	p.Y266C	yes	ND	F, D
3	F	3 months	29 [1.6]	4 [28]	246 [144]	*GLUD1*	c.1336G>A	p.G446S	Yes	ND	F, D
4	M	10 months	<45 [2.5]	7.7 [53]	154 [90]	*GLUD1*	c.1229A>G	p.N410S	No	ND	F, D
5	M	0 d	10 [0.6]	10 [69]	250 [147]	*GLUD1*	c.1229A>C	p.N410T	Yes	ND	F, D
6[a]	F	2 d	31 [1.7]	30.2 [210]	78 [46]	*ABCC8*	c.382G>A c.3748C>T	p.E128K p.R1250X	Yes, Yes	Biparental	
7	M	2 d	5 [0.3]	7.5 [52]	131 [77]	*ABCC8*	c.2506C>T c.4575_4587del13	p.R836X p.M1524Mfs1539X	Yes, No	Biparental	F, O
8	M	0 d	<45 [2.5]	11 [76]	58 [34]	*ABCC8*	c.4516G>A	p.E1506K	Yes	Mat	F, D
9[a]	F	1 month	<20 [1.1]	42.4 [294]	NA	*ABCC8*	c.2506C>T	p.R836X	Yes	Pat	
10[a]	M	2 d	10 [0.56]	23.5 [163]	NA	*ABCC8*	c.4412-13G>A	—	Yes	Pat	
11[a]	F	0 d	33 [1.8]	46.6 [324]	79 [46]	*ABCC8*	c.3745G>T	p.V1249F	No	Pat	
12[a]	F	3 months	20 [1.1]	5.16 [36]	78 [46]	*ABCC8*	c.2992C>T	p.R998X	Yes	Pat	
13[a]	F	0 d	23 [1.3]	101 [701]	45 [24]	*ABCC8*	c.4608 + 1G>A	—	No	Pat	
14[a]	M	0 d	22 [1.2]	22.7 [158]	75 [44]	*ABCC8*	c.2992C>T	p.R998X	Yes	Pat	
15[a]	M	5 months	33 [1.8]	5.42 [38]	NA	*ABCC8*	c.2992C>T	p.R998X	Yes	Pat	
16[a]	M	0 d	28 [1.6]	38.7 [269]	66 [39]	*ABCC8*	c.331G>A	p.G111R	Yes	Pat	
17	F	2 months	15 [0.8]	9.9 [69]	90 [53]	*ABCC8*	c.61_62insG	p.V21Gfs88X	No	Pat	F, O
18	M	0 d	19.6 [1.1]	44 [306]	79 [46]	*ABCC8*	c.2506C>T	p.R836X	Yes	Pat	F, O
19	F	7 months	35 [1.9]	11.2 [78]	97 [57]	*ABCC8*	c.2506C>T	p.R836X	Yes	Pat	F, O
20	M	4 months	<45 [2.5]	7.5 [52]	84 [49]	*ABCC8*	c.3928_3929insG	p.A1310Gfs1405X	No	Pat	F, O
21	M	2 d	38 [2.1]	3.4 [24]	91 [53]	*ABCC8*	c.4186G>T	p.D1396Y	No	Pat	F
22	F	0 d	9 [0.5]	22 [153]	NA	*ABCC8*	c.2506C>T	p.R836X	Yes	Pat	F, O
23	M	2 d	0 [0]	17.3 [120]	317 [186]	*ABCC8*	c.4412-13G>A	—	Yes	Pat	F, D
24[a]	M	0 d	33 [1.8]	21.9 [152]	75 [44]	*KCNJ11*	c.637G>A	p.A213T	No	Pat	

The clinical data are those at the initial presentation. Of the medically treated patients with monoallelic, paternally inherited K_{ATP} channel mutations (patients 17–23), none reported a family history of hypoglycemia. F, Frequent feeding; D, diazoxide; O, continuous sc injection of octreotide; M, male; F, female; Pat, paternal; Mat, maternal; NA, not available; ND, not determined.

[a] Patients who underwent surgery.

other 17 had monoallelic mutations. Furthermore, 16 of 17 of the mutations were of paternal origin. The single maternally inherited mutation was identical to a mutation previously reported by Huopio *et al.* (12) as a mutation causing hyperinsulinism in infancy and diabetes mellitus in adulthood. In fact, the mother of the patient developed diabetes at the age of 13 yr, and the maternal grandmother developed a mild form of diabetes during adulthood. Therefore, from the results of the mutational analyses, the incidence of a paternally inherited monoallelic mutation suggesting the presence of a focal lesion appears to be much higher in Japanese (84.2% of K_{ATP} channel hyperinsulinism cases).

Clinical studies and LCM studies

None of the patients with paternally inherited K_{ATP} channel mutations responded to diazoxide except for patient 23 who partially responded at the maximal dose of 25 mg/kg · d. Pancreatectomy was performed on 10 patients who were resistant to medical therapy, one with a biallelic *ABCC8* mutation (patient 6) and nine with monoallelic paternally inherited mutations, eight in *ABCC8* (patients 9–16), and one in *KCNJ11* (patient 24). [18F]-DOPA PET scans were performed in all patients preoperatively. The patient with the biallelic mutation (patient 6) showed typical diffuse uptake. Of the nine patients with monoallelic mutations, four showed a single focal uptake pattern (patients 9, 12, 15, and 16); two (patients 14 and 24) showed multifocal uptake; and the other three (patients 10, 11, and 13) showed irregular uptake throughout the pancreas, which was difficult to distinguish from that o diffuse lesions. The six patients with focal or multifocal uptake underwent partial resection of the pancreas. Histological examination revealed a single focal lesion in these patients. Five were almost completely cured, and one showed residual but milder hypoglycemia. Of the three patients who demonstrated irregular uptake during the PET study, two underwent subtotal pancreatectomy because their intraoperative findings did not rule out the presence of diffuse lesions. In one of these two patients (patient 13), postoperative histology revealed a large focal lesion in the tail and the body of the pancreas. In the other patient (patient 11), abnormal islets were found throughout the pancreas. The presence of normal islets in part of the pancreas suggested the diagnosis of a giant focal lesion. In the third patient (patient 10) with irregular [18F]-DOPA uptake (Fig. 1B), an arterial stimulation venous sampling study suggested the presence of a lesion in the body or the tail of the pancreas (Fig. 1A). Intraoperatively, no focal lesion could be identified by inspection or palpation. Although the margins of the lesion could not be clearly determined, partial resection was performed at 2.5 cm from the tail. This patient was also clinically cured after surgery. Postoperative histology revealed scattered, relatively large islets with a diameter of up to 700 μm clustered within the tail and the body. Each islet appeared to be separated by normal acinar cells, and no

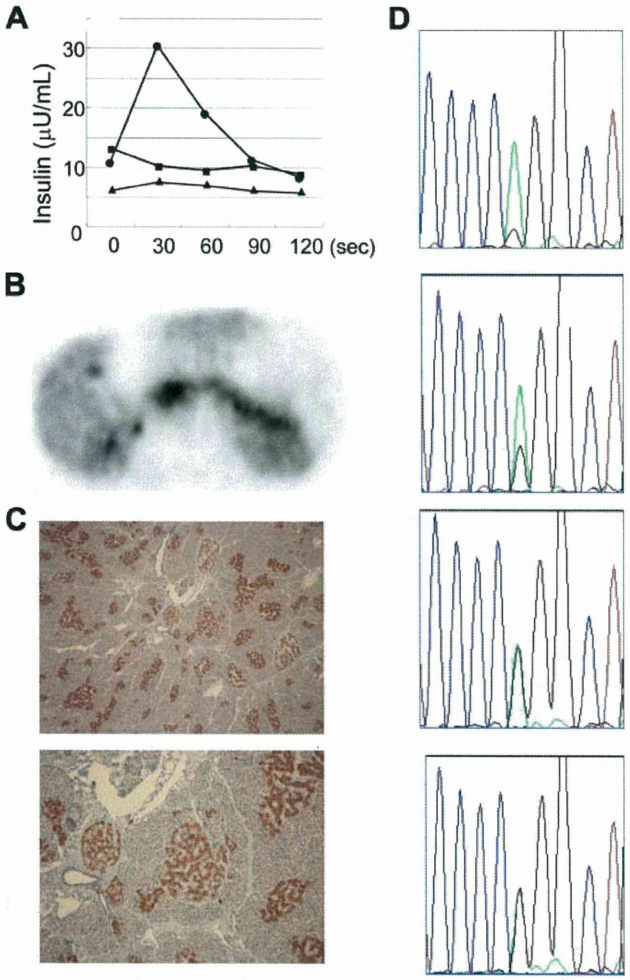

FIG. 1. Results of different diagnostic modalities in patient 10. A, Results of arterial stimulation venous sampling studies. The insulin concentration of the right hepatic vein was measured after the injection of calcium into the splenic (*filled circles*), gastroduodenal (*filled rectangles*), and superior mesenteric (*filled triangles*) arteries. An insulin response was observed only after stimulation of the splenic artery. B, A curved planar reconstruction of a [18F]-DOPA PET scan. The uptake in the head probably reflects an artifact. C, Chromogranin A staining of the resected pancreas showing the area in which abnormal islets were most densely distributed. Magnification, ×40 (*upper panel*), ×80 (*lower panel*). D, Mutational analysis of abnormal islet samples. The *upper two panels* show the results of two separate analyses of 30 (*upper panel*) and 40 (*lower panel*) islet samples. The *lower two panels* show the results of a similar analysis of an adjacent normal pancreatic area. The paternally inherited A allele (*green*) predominates in the abnormal islets, whereas the A and the wild-type G alleles (*black*) have similar intensities in the normal area of the pancreas.

single lesion composed of a solid β-cell cluster was identified by serial sections of the specimen (Fig. 1C). LCM was performed twice to collect samples from 30 and 40 of these islet clusters. Mutational analysis of the pooled DNA collected from these LCM samples revealed the predominance of the paternally inherited mutant allele within these scattered large islets compared with the surrounding normal pancreatic tissue (Fig. 1D).

Discussion

The most important finding of this study is the higher incidence of paternally inherited, monoallelic K_{ATP} channel mutations in Japanese patients with congenital hyperinsulinism ($P < 0.005$ by the sign test), which suggests that the majority of Japanese patients have the focal form. Although the number of patients is small, we believe our results represent the situation of the whole country for several reasons. First, a national survey in 2008–2009 conducted by the Ministry of Health, Labor, and Welfare of Japan estimated the incidence of persistent congenital hyperinsulinism as 1:35,400 births. Our study captured 23% of all cases during that period. Second, the patients were referred without geographical biases because ours is the only laboratory currently offering a comprehensive molecular diagnosis in Japan. Third, a previous report by Ohkubo *et al.* (13) also reported a high frequency (seven of 10) of monoallelic mutations in Japan. In contrast, patients with hyperinsulinism-hyperammonemia syndrome were collected somewhat arbitrarily over a longer period; therefore, the apparent higher incidence might not represent the actual incidence in Japan.

Conflicting results have been reported for the diabetogenesity of p.E1506K in *ABCC8* (12, 14, 15). The association might be a chance observation or might reflect a difference in the genetic background. If the association does exist, that might be due to the specific nature of the mutation, which confers the instability of the β-cells such as altered membrane potential of the cells.

Molecular diagnosis correctly predicted the histology in all patients who underwent pancreatectomy. On the contrary, the ability of [18F]-DOPA PET scans to identify focal lesions was inferior compared with the results of previous reports for other populations (16, 17). Histologically, at least two patients with ambiguous PET results had large focal lesions. The third patient (patient 10) appeared to have unusually scattered islets for a focal lesion. However, there remains the possibility that these islets are actually interconnected and represents a focal lesion with greater admixture of exocrine tissues. Although the number of patients was too small to draw a definite conclusion, larger lesions might be more common in the Japanese.

The reason that the incidence of the focal form of the disease is higher in Japanese is unclear. One possibility is that Japanese have a higher incidence of somatic isodisomy. If this occurred during the earlier stages of development, it would lead to the development of Beckwith-Wiedemann syndrome. However, the incidence of this syndrome caused by paternal isodisomy is not particularly higher in Japanese (18). Alternatively, cells with mutations common in Japanese might be more prone to develop into

a focal lesion, by either promoting a second hit of isodisomy or conferring a growth advantage after the disomic event. Further studies are necessary to address this question.

Acknowledgments

We thank Dr. Mariko Suchi (Children's Hospital of Wisconsin) for making an important suggestion about the pathological nature of atypical cases. We also thank the following physicians for referring the patients to us and for their helpful discussion: Drs. Reiko Horikawa (National Center for Child Health and Development); Toshiyuki Fukao (Gifu University); and Koji Muroya and Masanori Adachi (Kanagawa Children's Medical Center).

Address all correspondence and requests for reprints to: Tohru Yorifuji, M.D., Ph.D., Department of Pediatric Endocrinology and Metabolism, Osaka City General Hospital, 2-13-22 Miyakojima-Hondori, Miyakojima, Osaka 534-0021, Japan. E-mail: t-yorifuji@hospital.city.osaka.jp.

This work was supported by Grant-in-Aid for Scientific Research (Research on Measures for Intractable Diseases 2009-189 and 2010-101) from the Ministry of Health, Labor, and Welfare of Japan.

Disclosure Summary: No conflict of interests is declared.

References

1. De León DD, Stanley CA 2007 Mechanisms of disease: advances in diagnosis and treatment of hyperinsulinism in neonates. Nat Clin Pract Endocrinol Metab 3:57–68
2. Meissner T, Wendel U, Burgard P, Schaetzle S, Mayatepek E 2003 Long-term follow-up of 114 patients with congenital hyperinsulinism. Eur J Endocrinol 149:43–51
3. Menni F, de Lonlay P, Sevin C, Touati G, Peigné C, Barbier V, Nihoul-Fékété C, Saudubray JM, Robert JJ 2001 Neurologic outcomes of 90 neonates and infants with persistent hyperinsulinemic hypoglycemia. Pediatrics 107:476–479
4. Leibowitz G, Glaser B, Higazi AA, Salameh M, Cerasi E, Landau H 1995 Hyperinsulinemic hypoglycemia of infancy (nesidioblastosis) in clinical remission: high incidence of diabetes mellitus and persistent beta-cell dysfunction at long-term follow-up. J Clin Endocrinol Metab 80:386–392
5. Verkarre V, Fournet JC, de Lonlay P, Gross-Morand MS, Devillers M, Rahier J, Brunelle F, Robert JJ, Nihoul-Fékété C, Saudubray JM, Junien C 1998 Paternal mutation of the sulfonylurea receptor (SUR1) gene and maternal loss of 11p15 imprinted genes lead to persistent hyperinsulinism in focal adenomatous hyperplasia. J Clin Invest 102:1286–1291
6. de Lonlay P, Fournet JC, Rahier J, Gross-Morand MS, Poggi-Travert F, Foussier V, Bonnefont JP, Brusset MC, Brunelle F, Robert JJ, Nihoul-Fékété C, Saudubray JM, Junien C 1997 Somatic deletion of the imprinted 11p15 region in sporadic persistent hyperinsulinemic hypoglycemia of infancy is specific of focal adenomatous hyperplasia and endorses partial pancreatectomy. J Clin Invest 100:802–807
7. Glaser B, Ryan F, Donath M, Landau H, Stanley CA, Baker L, Barton DE, Thornton PS 1999 Hyperinsulinism caused by paternal-specific inheritance of a recessive mutation in the sulfonylurea-receptor gene. Diabetes 48:1652–1657
8. Damaj L, le Lorch M, Verkarre V, Werl C, Hubert L, Nihoul-Fékété C, Aigrain Y, de Keyzer Y, Romana SP, Bellanne-Chantelot C, de Lonlay P, Jaubert F 2008 Chromosome 11p15 paternal isodisomy in focal forms of neonatal hyperinsulinism. J Clin Endocrinol Metab 93:4941–4947
9. Fernández-Marmiesse A, Salas A, Vega A, Fernández-Lorenzo JR, Barreiro J, Carracedo Á 2006 Mutation spectra of ABCC8 gene in Spanish patients with hyperinsulinism of Infancy (HI). Hum Mutat 27:214
10. Sandal T, Laborie LB, Brusgaard K, Eide SA, Christesen HB, Søvik O, Njølstad PR, Molven A 2009 The spectrum of ABCC8 mutations in Norwegian patients with congenital hyperinsulinism of infancy. Clin Genet 75:440–448
11. Ribeiro MJ, De Lonlay P, Delzescaux T, Boddaert N, Jaubert F, Bourgeois S, Dollé F, Nihoul-Fékété C, Syrota A, Brunelle F 2005 Characterization of hyperinsulinism in infancy assessed with PET and 18F-fluoro-L-DOPA. J Nucl Med 46:560–566
12. Huopio H, Otonkoski T, Vauhkonen I, Reimann F, Ashcroft FM, Laakso M 2003 A new subtype of autosomal dominant diabetes attributable to a mutation in the gene for sulfonylurea receptor 1. Lancet 361:301–307
13. Ohkubo K, Nagashima M, Naito Y, Taguchi T, Suita S, Okamoto N, Fujinaga H, Tsumura K, Kikuchi K, Ono J 2005 Genotypes of the pancreatic β-cell K-ATP channel and clinical phenotypes of Japanese patients with persistent hyperinsulinemic hypoglycemia of infancy. Clin Endocrinol (Oxf) 62:458–465
14. Pinney SE, MacMullen C, Becker S, Lin YW, Hanna C, Thornton P, Ganguly A, Shyng SL, Stanley CA 2008 Clinical characteristics and biochemical mechanisms of congenital hyperinsulinism associated with dominant K_{ATP} channel mutations. J Clin Invest 118:2877–2886
15. Vieira TC, Bergamin CS, Gurgel LC, Moisés RS 23 December 2009 Hyperinsulinemic hypoglycemia evolving to gestational diabetes and diabetes mellitus in a family carrying the inactivating ABCC8 E1506K mutation. Pediatr Diabetes 10.1111/j.1399-5448.2009.00626.x
16. Hardy OT, Hernandez-Pampaloni M, Saffer JR, Suchi M, Ruchelli E, Zhuang H, Ganguly A, Freifelder R, Adzick NS, Alavi A, Stanley CA 2007 Diagnosis and localization of focal congenital hyperinsulinism by 18F-fluorodopa PET scan. J Pediatr 150:140–145
17. Mohnike K, Blankenstein O, Minn H, Mohnike W, Fuchtner F, Otonkoski T 2008 [18F]-DOPA positron emission tomography for preoperative localization in congenital hyperinsulinism. Horm Res 70:65–72
18. Sasaki K, Soejima H, Higashimoto K, Yatsuki H, Ohashi H, Yakabe S, Joh K, Niikawa N, Mukai T 2007 Japanese and North American/European patients with Beckwith-Wiedemann syndrome have different frequencies of some epigenetic and genetic alterations. Eur J Hum Genet 15:1205–1210

World J Surg (2011) 35:393–402
DOI 10.1007/s00268-010-0869-6

World Journal of Surgery

Living-donor Liver Transplantation for Progressive Familial Intrahepatic Cholestasis

Tomohide Hori · Hiroto Egawa · Aya Miyagawa-Hayashino · Tohru Yorifuji · Yukihide Yonekawa · Justin H. Nguyen · Shinji Uemoto

Published online: 2 December 2010

Abstract
Background Progressive familial intrahepatic cholestasis (PFIC) results in liver cirrhosis during the disease course, although the etiology includes unknown mechanisms. Some PFIC patients require liver transplantation (LT).
Methods In this study, 11 patients with PFIC type 1 (PFIC1) and 3 patients with PFIC type 2 (PFIC2) who underwent living-donor LT (LDLT) were evaluated.
Results Digestive symptoms after LDLT were confirmed in 10 PFIC1 recipients (90.9%); 8 PFIC1 recipients showed steatosis after LDLT (72.7%), which began during the early postoperative period (71.5 ± 55.1 days). Seven of the eight steatosis-positive PFIC1 recipients (87.5%) showed a steatosis degree of ≥80%, which was complicated with steatohepatitis and resulted in fibrosis. Cirrhotic findings persisted in six PFIC1 recipients even after LDLT (54.5%), and three PFIC1 recipients finally died. The survival rates of the PFIC1 recipients at 5, 10, and 15 years were 90.9%, 72.7%, and 54.5%, respectively. In contrast, the PFIC2 recipients showed good courses and outcomes without any steatosis after LDLT.
Conclusions The clinical courses and outcomes after LDLT are still not sufficient in PFIC1 recipients owing to steatosis/steatohepatitis and subsequent fibrosis, in contrast to PFIC2 recipients. PFIC2 is good indication for LDLT. PFIC1 patients require LT during the disease course; therefore, we suggest that the therapeutic strategies for PFIC1 patients, including the timing of LDLT, under the donor limitation should be reconsidered. The establishment of more advanced treatments for PFIC1 patients is required to improve the long-term prognosis of these patients.

T. Hori (✉) · H. Egawa · S. Uemoto
Division of Hepato-Biliary-Pancreatic and Transplant Surgery, Department of Surgery, Kyoto University Hospital, 54 Shogoinkawara-cho, Sakyo-ku, Kyoto 606-8507, Japan
e-mail: horit@kuhp.kyoto-u.ac.jp

A. Miyagawa-Hayashino
Department of Diagnostic Pathology, Kyoto University Hospital, Kyoto 606-8507, Japan

T. Yorifuji
Department of Pediatrics, Kyoto University Hospital, Kyoto 606-8507, Japan

Y. Yonekawa · S. Uemoto
Division of Pediatric Surgery, Department of Surgery, Kyoto University Hospital, Kyoto 606-8507, Japan

J. H. Nguyen
Division of Transplant Surgery, Department of Transplantation, Mayo Clinic Florida, Jacksonville, FL 32224, USA

Introduction

Progressive familial intrahepatic cholestasis (PFIC) refers to a heterogeneous group of autosomal recessive disorders of childhood that disrupt bile formation and present with cholestasis. PFIC is a rare disease, with an estimated incidence of 1 per 50,000–100,000 births [1]. Cholestasis of hepatocellular origin is the major sign in PFIC. The cholestasis appears within the first year of life and leads to death from liver failure at ages from infancy to adolescence [2, 3]. Although the etiology of PFIC still involves unknown mechanisms, the natural course of PFIC causes portal hypertension, liver failure, cirrhosis, carcinoma, and extrahepatic disorders.

PFIC is classified into three types as follows: (1) deficiency of familial intrahepatic cholestasis 1 (FIC1); (2) deficiency of bile salt export pump (BSEP); (3) deficiency of multidrug-resistant 3 (MDR3). Mutations in these genes

are related to the hepatocellular transport system involved in bile formation. The clinical, biochemical, radiological, and histological manifestations of each type have been described previously [1–11].

In PFIC type 1 (PFIC1) patients, cholestasis appears during the first months of life and causes recurrent episodes of jaundice that eventually become permanent. Severe pruritus is observed. The serum γ-glutamyltransferase (γ-GT) and cholesterol levels are normal, but the bile acid (BA) concentration is high. The hepatic histopathology is characterized by canalicular cholestasis and the absence of true ductular proliferation. PFIC1 is caused by mutations in the *ATP8B1* gene, which is designated FIC1 [6–12]. FIC1 is expressed in the liver, pancreas, small intestine, and kidney. The FIC1 protein is located on the canalicular membrane of hepatocytes [13–15]. FIC1 is more highly expressed in the small intestine than in the liver [12]. Taken together, these events lead to BA overload in hepatocytes, impaired bile secretion in cholangiocytes, and extrahepatic features in the intestine [1, 6, 14, 16]. Extrahepatic symptoms (persistent short stature, sensorineural deafness, watery diarrhea, pancreatitis, elevated sweat electrolyte concentration) have been confirmed in PFIC1 patients [9], and enterohepatic circulation should be considered in PFIC1.

Cholestasis with permanent jaundice is more severe in PFIC type 2 (PFIC2) patients than in those with the other PFIC types, although PFIC2 patients share similar laboratory findings with PFIC1 patients. The initial evolution of cholestasis appears during the first months of life and rapidly results in liver failure within the first few years of life. More severe pruritus is observed. The histopathological findings reveal more perturbed liver architecture than is seen in PFIC1, with more pronounced lobular and portal fibrosis and inflammation [2, 8, 9]. PFIC2 is caused by mutations in the *ABCB11* gene, which is designated BSEP [7, 17]. This gene encodes the ATP-dependent canalicular BSEP of the liver. The BSEP protein, which is expressed at the hepatocyte canalicular membrane, is the major exporter of primary BA against extreme concentration gradients. Mutations in this gene are responsible for decreased the secretion of bile salts (BSs), leading to decreased bile flow and accumulation of BSs inside the hepatocytes, which results in severe hepatocellular damage. Extrahepatic features have not been documented in PFIC2. However, hepatocellular carcinoma (HCC) and cholangiocarcinoma occurs at a considerable rate (15%) before 1 year of age [18, 19].

PFIC type 3 (PFIC3) patients show high γ-GT, normal cholesterol, and slightly elevated BA levels. PFIC3 can be distinguished from the other PFICs, because it rarely appears during the neonatal period but manifests during infancy, childhood, and even young adulthood [11, 20]. Pruritus is mild, and the evolution of cholestasis is chronic icteric or anicteric. Therapy with ursodeoxycholic acid (UDCA) may be especially effective for PFIC3 [1, 11, 21].

Regardless of the various types, PFIC patients develop hepatic failure and liver cirrhosis during the disease course. Therefore, it is currently justified that PFIC patients undergo liver transplantation (LT). Here, we present our results for PFIC patients after living-donor LT (LDLT) during two decades and discuss therapeutic strategies for PFIC patients.

Patients and methods

Patients

Since 1990, a total of 735 adult and 702 pediatric recipients underwent LT at Kyoto University Hospital. In all, 717 LDLT recipients whose ages at LDLT were <20 years were enrolled in this study. Among the LDLT recipients, 11 PFIC1 and 3 PFIC2 recipients were evaluated (Table 1); there were no LDLTs in PFIC3 patients. The Ethics Review Committee for Clinical Studies at Kyoto University Graduate School of Medicine approved the study protocol.

The 14 PFIC patients comprised five males and nine females, and their age range at LDLT was 0.6–18.2 years. The mean times from the diagnosis of PFIC to LDLT were 3.89 ± 5.63 years (range 0.21–16.3 years) for the PFIC1 recipients and 0.79 ± 0.75 years (range 0.12–1.60 years) for the PFIC2 recipients. The standard deviation (SD) values for height and body weight at LDLT were −4.5 ± 1.8 (range −7.5 to -1.1) and −2.1 ± 1.0 (range −3.5–0.3), respectively. Growth retardation was confirmed in all patients. One PFIC1 patient (case 5) had a past history of paroxysmal atrial fibrillation.

The serum total BA level was elevated to 439.1 ± 109.8 μmol/ml (range 299–600 μmol/ml), and the γ-GT level was normal at 16.6 ± 4.0 IU/L (range 12–26 IU/L). The mean Child-Pugh score was 7.9 ± 0.8 points (range 7–9 points). The mean score of the Model for End-stage Liver Disease (ages ≥12 years) or Pediatric End-stage Liver Disease (ages <12 years) was 12.3 ± 4.1 points (range 5–19 points). The preoperative statuses were 11 cases of at home and 3 cases of hospitalization. The United Network for Organ Sharing statuses were estimated to be 12 cases of status III and two cases of status IIB.

The donor relationships were 10 fathers, 3 mothers, and 1 grandmother. The mean donor age was 36.9 ± 7.1 years (range 28–47 years). The mean body mass index (BMI) in the donors was 22.3 ± 1.0 kg/m^2 (range 20.5–23.6 kg/m^2). One donor (case 8) was hepatitis B surface antibody (HBsAb)-positive. The ABO blood groups were

Table 1 Histopathological findings after LDLT

Case no.	Steatosis	Steatohepatitis	Fibrosis score (F)[a]	Other factors for fibrosis
PFIC type 1				
1	Severe	Yes	3	–
2	None	No	4	De novo AIH
3	Severe	Yes	4	–
4	None	No	0	–
5	Severe	Yes	3	–
6	Severe	Yes	3	–
7	Moderate	Yes	4	–
8	Severe	No	0	–
9	Severe	Yes	3	–
10	None	No	4	Chronic rejection
11	Severe	Yes	1	–
PFIC type 2				
12	None	Yes	0	–
13	None	Yes	0	–
14	None	Yes	0	–

AIH Autoimmune hepatitis, *LDLT* living-donor liver transplantation, *NASH* nonalcoholic steatohepatitis, *PFIC* progressive familial intrahepatic cholestasis

[a] The NASH score was used in steatosis-positive recipients. The Metavir score was used in steatosis-negative recipients

characterized as 11 cases identical, 2 cases compatible and 1 case incompatible (case 13). The results of lymphocyte crossmatches were negative.

Operation

There were 12 lateral-segment grafts and one case each of extended lateral-segment and left-lobe grafts. The mean graft/recipient weight ratio was 2.08 ± 0.91 (range 1.20–4.02). Histopathological analyses of biopsy specimens during the donor operation were performed in seven cases, and normal findings were confirmed. The mean operating time was 525.4 ± 57.4 min (range 402–636 min), and the mean blood loss was 949.3 ± 833.9 ml (range 105–2610 ml). The mean cold and warm ischemia times were 51.0 ± 29.4 min (range 15–99 min) and 35.9 ± 11.6 min (range 24–56 min), respectively. Biliary reconstruction at the initial LDLT was done by hepaticojejunostomy in 12 cases and by duct-to-duct reconstruction in 2 cases (cases 8 and 14). Histopathologically, cirrhosis without steatosis was confirmed in all of the native livers.

Immunosuppression

Immunosuppression after LDLT was started with tacrolimus and methylprednisolone. The trough level of tacrolimus was maintained at 8–15 ng/ml during the early postoperative period based on the clinical findings in each case. Methylprednisolone was given intravenously (1 mg/kg) once daily from postoperative day (POD) 1 to POD 3 followed by 0.5 mg/kg once daily for the next 3 days. On POD 7, methylprednisolone 0.3 mg/kg was given intravenously. Steroid administration was switched to oral prednisolone 0.3 mg/kg once daily on POD 8. Our regimens for ABO incompatibility were described previously [22, 23].

Histopathological analysis

In our institution, laboratory and ultrasonography (US) examinations are performed routinely after LDLT in all recipients. A liver needle biopsy (LNB) was performed if required based on the results of conventional liver function tests, findings of Doppler US, and consideration of the original diseases. All LNB specimens were strictly assessed by experienced pathologists.

All liver tissues were fixed in neutral-buffered formalin, embedded in paraffin, and sliced into 4 μm thick sections. The morphological characteristics were assessed after standard hematoxylin-eosin (H&E) staining, and hepatic fibrosis was reconfirmed by Masson trichrome and reticulin staining.

Posttransplant steatosis was evaluated as the percentage of hepatocytes involved in steatosis in the liver tissue [24]. Macrovesicular steatosis was graded semiquantitatively according to the percentage of involved hepatocytes as follows [24]: mild <30% of hepatocytes; moderate 30% to 60% of hepatocytes; severe >60% of hepatocytes. The diagnosis of steatohepatitis was defined according to any degree of steatosis, hepatocellular injury in the form of ballooning degeneration and/or Mallory's hyaline, mononuclear and polymorphonuclear infiltration, perisinusoidal fibrosis and portal/lobular inflammation. The fibrosis scores were strictly estimated based on the presence or absence of posttransplant steatosis. Estimation of the hepatic venous area is important at the early phase